

## Carbon–Oxygen Bond Dissociation Enthalpies in Peroxyl Radicals

Marieke Kranenburg,<sup>†</sup> Maria Victoria Ciriano,<sup>†</sup> Artem Cherkasov,<sup>‡</sup> and Peter Mulder<sup>\*,†</sup>*Leiden Institute of Chemistry, Leiden University, PO Box 9502, 2300 RA Leiden, The Netherlands, and the Department of Chemistry, Nuclear Chemistry, Royal Institute of Technology, SE-10044 Stockholm, Sweden**Received: July 15, 1999; In Final Form: October 12, 1999*

The reaction enthalpies for the recombination of carbon-centered radicals, R•, with molecular oxygen have been established by photoacoustic calorimetry (PAC) in the liquid phase and by means of density functional theory calculations (DFT) with the B3LYP functionals and the 6-31(d) basis set. The experimental study revealed the following carbon–oxygen bond dissociation enthalpies, BDE(R–OO) (kcal mol<sup>-1</sup>): cyclohexadienyl (12), 1-tetrahydrofuryl (32), and dioxanyl (34). For 1-triethylaminyl and 1-pyrrolidinyl, the reaction enthalpy suggests that in organic solvents disproportionation becomes important even within the first stage of the reaction. DFT underestimates the BDE(R–OO) by 0–6 kcal mol<sup>-1</sup>. However, DFT BDE(R–H)–BDE(R–OO) are in accordance with experimental data. The computed BDE(R–OO) is not sensitive to substitution by alkyl groups.

## Introduction

The interaction of oxygen with organic matter is probably the most abundant chemical process known to man. It is essential in the production of thermal energy, but at the same time, it is responsible for the unwanted deterioration of polymers, lubricating oils, and cellular membranes. It is well documented that this oxidative breakdown proceeds according to a radical chain mechanism. In liquids, the carbon-centered radical is trapped by molecular oxygen (eq 1) at a near diffusion-controlled rate.<sup>1</sup>



Subsequently, the organic peroxy radical abstracts a hydrogen atom from the organic material as the rate-determining step (eq 2) to support the radical chain.



In principle, as for any radical–radical process, two product-forming steps can be discerned: recombination (eq 1) or disproportionation (eq 3) to yield an alkene and the hydro-



peroxy radical. It is generally accepted that at ambient temperature recombination with oxygen is the sole pathway. At elevated temperatures, the disproportionation gains in importance due to the reverse of eq 1, the decomposition of ROO•, in which the rate is entirely governed by the magnitude of the carbon–oxygen bond dissociation enthalpy, BDE(R–OO).

In the gas phase, the pathways for the ethyl radical with molecular oxygen have been extensively studied by experimental and computational methods. The unexpected formation of ethene at low temperatures and pressures can be rationalized by considering either a hydrogen transfer followed by elimination

of HO<sub>2</sub>• or a direct HO<sub>2</sub>• expulsion starting from the (excited) ethylperoxy radical.<sup>2</sup>

Despite their importance, only a few gas-phase BDE(R–OO)s have been determined experimentally; for alkyl species, the BDE(R–OO)s ranges 33–37 kcal mol<sup>-1</sup>.<sup>3</sup> Contrary to carbon–hydrogen or carbon–carbon bonds, the influence by substituents, other than alkyl, on the carbon–oxygen energetics has not been studied in a systematic fashion. The carbon–oxygen linkage is polarized, and upon substitution by groups containing an electronegative element like OR or NHR, an additional electronic interaction may be anticipated. Recently, we have demonstrated that the strength of the bond formed between the 1-tetrahydrofuryl and an organic nitroxide, (2,2,6,6-tetramethylpiperidine-1-oxyl) is strongly influenced by stereoelectronic factors.<sup>4</sup>

Therefore, we embarked on a study to determine the heat of eq 1 for some prototypical radicals by means of photoacoustic calorimetry (PAC). A laser induced chemical reaction causes an acoustic shock wave and the change in pressure is proportional to the heat released. This thermodynamic method monitors the enthalpic change within the submicrosecond domain.<sup>5</sup>

Furthermore, a computational study employing a density functional theory (DFT) with the B3LYP functionals on the 6-31(d) level has been carried out to predict the BDE(R–H) and the BDE(R–OO) for a larger set of compounds.

## Experimental Section

**Materials.** All chemicals were obtained from commercial sources in the purest available grade. Spectrograde solvents were distilled before use, except 1,4-cyclohexadiene, which was used as received. 2-Hydroxybenzophenone was crystallized twice from ethanol, and di-*tert*-butyl peroxide (*t*-BuOOBu-*t*) was passed over activated alumina before use. Dicumylhyponitrite was synthesized from cumyl chloride and silverhyponitrite as reported before.<sup>6</sup> Silverhyponitrite was synthesized from sodiumhyponitrite and silvernitrate. Silvernitrate (15 g) was dissolved in 150 mL of water and cooled to 273 K. A solution of 3 g of sodium hyponitrite in 100 mL of water was added dropwise during 3 h in the dark while stirring, and the final

\* To whom correspondence should be addressed. E-mail: p.mulder@chem.leidenuniv.nl. Fax: (31)-71-5274492.

<sup>†</sup> Leiden University.

<sup>‡</sup> Royal Institute of Technology.

solution was kept for another 1.5 h at 273 K. Subsequently, the silverhyponitrite was filtered, washed with 3.5 L of water and dried over P<sub>2</sub>O<sub>5</sub>. All other chemicals were used as received.

**Photoacoustic Calorimetry.** The photoacoustic apparatus consists of a modified fluorescence cuvette (Hellma 221), to allow continuous flow experiments, containing solutions of di-*tert*-butyl peroxide and the compound of interest. After deoxygenation by purging with argon or saturation with oxygen, the solutions were photolyzed using 600 ps pulses from a PRA LN 1000 nitrogen laser (337.1 nm, 84.8 kcal mol<sup>-1</sup>). The resulting shock wave was detected by a Panametrics model V101, 1 MHz, piezo electric transducer clamped to the bottom of the cell (with a thin layer of vacuum grease to provide good acoustic transmission). The signals were amplified (Panametrics model 5670 ultrasonic preamp) and digitized (Tektronix model 2430A Digital Oscilloscope). The signal-to-noise ratio was improved to up to 100:1 by averaging 256 acquisitions. Each data point was determined three times. Fluctuations in the laser energy were monitored using an L-PED pyroelectric device to which 10% of the incident laser beam was directed. The remaining radiation was passed through a 1 mm pinhole in front of the cuvette. The average laser energy in these experiments was <50 mJ/pulse (i.e., flux < 6 mJ/cm<sup>2</sup>). The photoacoustic cell was located inside an HP 8452A diode array spectrophotometer so that the absorbance (average of 10 recordings) of the solution could be measured simultaneously with the PAC signal.

A relative method is employed in which the photoacoustic signal,  $S_{\text{obs}}$ , is recorded (and normalized to allow for variations in the photon flux) as a function of the number of 337 nm photons absorbed by the sample ( $1 - 10^{-\text{OD}}$ ). The magnitude of  $1 - 10^{-\text{OD}}$  is altered by carrying out experiments using different concentrations of peroxide. A plot of  $S_{\text{obs}}$  then yields an excellent straight line ( $r^2 \geq 0.9998$ ) with a slope of  $a_{\text{obs}}$ . Under the same experimental conditions, the microphone response is calibrated using *o*-hydroxybenzophenone, which absorbs at 337 nm and converts all the absorbed energy to heat, in the same solvent (mixture) but without the peroxide. A plot of the photoacoustic signal,  $S_{\text{ref}}$ , vs ( $1 - 10^{-\text{OD}}$ ) yields the second slope:  $a_{\text{ref}}$  ( $r^2 \geq 0.9998$ ). Hence, the fraction of the photon energy released as heat is given by  $f_{\text{obs}} = a_{\text{obs}}/a_{\text{ref}}$ .

**Liquid-Phase Experiments.** The liquid-phase experiments (in duplicate) for the determination of the rate constants were carried out in neat liquid mixtures using sealed Pyrex tubes (ca. 1.5 mL). After filling the tube with about 0.5 mL of a solution of the reactants [typical concentrations: 0.25 M di-*tert*-butyl peroxide, 0.55 M 2,2,6,6-tetramethylpiperidine-1-oxyl (TEMPO)] and naphthalene as the internal standard, air was removed by three freeze-pump-helium-thaw cycles. The tube was sealed under vacuum and placed in a thermostat-controlled oven at 393 K for 16 h. After cooling to room temperature, the tube was decapped and dodecane was added as an external standard. Similar experiments were repeated with dicumylhyponitrite as the source for cumyloxyl radicals at 318 K for 7 h to allow for a complete decomposition of the hyponitrite.

The samples were analyzed in quadruplicate on an HP 5890A gas chromatograph with a CP-Sil-5-CB capillary column and hydrogen as the carrier gas. Products were identified on a GC-MS (HP 5890A-HP5972) with an HP-1MS column with helium as the carrier gas. Response factors relative to dodecane were calculated by injection of authentic samples. The response factors for the TEMPO adducts (N-alkoxylamines) were derived on the basis of additivity. The reproducibility of the analysis was >95%.

**DFT Calculations.** Geometries and vibrational frequencies were fully optimized to stationary points on the B3LYP/6-31-(d) level using a Gaussian 94W, rev. E.3, suite of programs and a PC (300 MHz or higher). Input Z-matrix for the geometry was obtained from a semiempirical PM3 calculation employing the HyperChem software package. The zero point vibrational energy (ZPVE) corrections were scaled by a factor 0.9806 to account for anharmonicity.<sup>7</sup> For the closed shell molecules and the radicals, the spin-restricted (R) and unrestricted (U) formalisms were used, respectively.

## Results

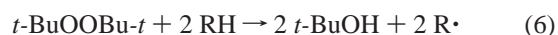
**Photoacoustic Calorimetry.** In a solution containing the compound of interest (RH) and di-*tert*-butyl peroxide, *tert*-butoxyl radicals are generated through photolysis at 337 nm by a pulsed nitrogen laser (eq 4); subsequently hydrogen abstraction



from RH takes place (eq 5). The overall chemical change is



given by eq 6. The observed reaction enthalpy for eq 6,  $\Delta_6 H_{\text{obs}}$ ,



is retrieved according to eq 7 by measuring the apparent fraction

$$\Delta_6 H_{\text{obs}} = \frac{E_{h\nu}}{\Phi} (1 - f_{\text{obs}}) \quad (7)$$

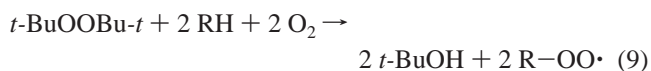
of photon energy,  $f_{\text{obs}}$ , released as heat.

In eq 7,  $E_{h\nu}$  is the nitrogen laser energy (84.8 kcal mol<sup>-1</sup>) and  $\Phi$  is the photochemical quantum yield for photodissociation of the peroxide (eq 4) in a particular solvent. The observed reaction enthalpy is not identical to  $\Delta_6 H$  as has been outlined before.<sup>5b</sup> Provided that the rate of hydrogen abstraction is fast enough, that is eq 5 is completed within 300 ns, the BDE(R-H) in RH can be calculated from eq 8. Equation 8 contains

$$\text{BDE}(\text{R-H}) = 0.5\Delta_6 H_{\text{obs}} - 0.5(\Delta\Delta H_{\text{soln}} - \Delta V_4/\chi_s) + 86.0 \quad (8)$$

$\Delta\Delta H_{\text{soln}}$  as the change in heats of solvation for converting one di-*tert*-butyl peroxide into two *tert*-butyl alcohols and  $\Delta V_4/\chi_s$  as the (positive) chemical volume change. The factor of 86.0 kcal mol<sup>-1</sup> equals the difference in heats of formation of  $0.5\Delta_f H_{298}(t\text{-BuOOBu-}t) - \Delta_f H_{298}(t\text{-BuOH}) + \Delta_f H_{298}(\text{H})$ .

By saturation of the solution with molecular oxygen, the formed radicals (eq 5) will be trapped to yield the peroxy radicals (eq 1). The overall chemical change is now represented by eq 9, and by PAC the  $\Delta_9 H_{\text{obs}}$  is determined.



The intensity of the PAC signal,  $S_{\text{obs}}$ , did not change when applying a gas stream for saturation of Ar/O<sub>2</sub> (1:1), showing that the oxygen concentrations<sup>8</sup> are sufficiently high to allow a quantitative heat deposition (i.e., the rates of eq 1 and 5 are fast enough).<sup>5c</sup> With triethylamine (TEA) in isooctane, and in the absence of peroxide, the absorption at 337 nm increased when the solution was purged with oxygen, with a concomitant increase of the PAC background signal. The signal increased linearly with the concentration of TEA suggesting the presence

**TABLE 1: BDE(R–H) and BDE(R–OO) (kcal mol<sup>-1</sup>) Determined by Photoacoustic Calorimetry<sup>a</sup>**

R	solvent	$\Phi$	$\Delta_6 H_{\text{obs}}$	BDE (R–H)	$\Delta_9 H_{\text{obs}}$	BDE (R–OO)
<i>c</i> -C <sub>6</sub> H <sub>11</sub> <sup>b</sup>	CHEX	0.78	12	97	-28	24 <sup>c</sup>
<i>c</i> -C <sub>6</sub> H <sub>7</sub> <sup>d</sup>	ISOC	0.83	-29	77	-45	12
	EA	0.86	-33	77	-51	13
<i>c</i> -C <sub>4</sub> H <sub>8</sub> N <sup>e</sup>	EA	0.86	-11	87 <sup>f</sup>	-24	10 <sup>c,g</sup>
(C <sub>2</sub> H <sub>5</sub> ) <sub>2</sub> NCHCH <sub>3</sub> <sup>h</sup>	ISOC	0.83	-4	89 <sup>i</sup>	-47	25 <sup>c</sup>
	EA	0.86	-8	89	-49	24 <sup>c</sup>
C <sub>4</sub> H <sub>7</sub> O <sup>j</sup>	THF	0.85	-2	92	-60	32 <sup>g</sup>
C <sub>4</sub> H <sub>7</sub> O <sub>2</sub> <sup>k</sup>	DIOX	0.74	7	96	-54	34 <sup>g</sup>

<sup>a</sup> BDEs based on at least two runs, error margins  $\pm 1.0$  kcal mol<sup>-1</sup>. Error margin  $\Delta H_{\text{obs}} = \pm 1-1.5$  kcal mol<sup>-1</sup>, uncertainties in numerical values (eq 8) =  $\pm 1$  kcal mol<sup>-1</sup>. ( $\Delta \Delta H_{\text{sol}} = \Delta \Delta H_{\text{sol}} - \Delta V_4/\chi_s$  (eq 8)). Cyclohexane (CHEX) and isooctane (ISOC): -10 kcal mol<sup>-1</sup>. Tetrahydrofuran (THF), 1,4-dioxane (DIOX), and ethyl acetate (EA): -13 kcal mol<sup>-1</sup>.  $\Phi$  is the photochemical quantum yield for photodissociation.<sup>5a</sup> <sup>b</sup> Cyclohexane: competition experiments with 0.3 M CHD and 8.9 M CHEX result in  $\Delta_6 H_{\text{obs}} = -13$  kcal mol<sup>-1</sup>.  $k_{5,\text{CHEX}} = 6.4 \times 10^5$  M<sup>-1</sup> s<sup>-1</sup> (see text) and  $k_{5,\text{CHD}} = 3 \times 10^7$  M<sup>-1</sup> s<sup>-1</sup> yields  $\xi = 0.39$ . Using  $\Delta_6 H_{\text{obs,CHD}} = -29$  kcal mol<sup>-1</sup> and eq 11 gives  $\Delta_6 H_{\text{obs,CHEX}} = 12$  kcal mol<sup>-1</sup>. With O<sub>2</sub>,  $\Delta_9 H_{\text{obs}} = -38$  kcal mol<sup>-1</sup> and  $\Delta_9 H_{\text{obs,CHEX}} = -28$  kcal mol<sup>-1</sup>. The same result has been found with a mixture of CHEX and phenol. However, with 3 M THF in 6.9 M CHEX,  $\Delta_9 H_{\text{obs}} = -62$  kcal mol<sup>-1</sup> was obtained. With  $\xi = 0.25$  and  $\Delta_9 H_{\text{obs,THF}} = -58$  kcal mol<sup>-1</sup>,  $\Delta_9 H_{\text{obs,CHEX}}$  becomes -74 kcal mol<sup>-1</sup>, leading to a BDE(R–OO) of 47 kcal mol<sup>-1</sup>. <sup>c</sup> This value does not reflect BDE(R–OO); see text. <sup>d</sup> 1,4-Cyclohexadiene, 0.5 M. <sup>e</sup> Pyrrolidine, 0.1 M. <sup>f</sup> A BDE(R–H) = 90.1  $\pm$  2 kcal mol<sup>-1</sup> has been reported by Wayner et al.<sup>10</sup> <sup>g</sup> The BDE(R–OO) has been corrected by adding 2 kcal mol<sup>-1</sup> to  $\Delta_9 H_{\text{obs}}$  due to solvation of the peroxy radical. <sup>h</sup> Triethylamine, 0.5 M in isooctane and 0.5 and 0.1 M in ethyl acetate. <sup>i</sup> A BDE(R–H) = 90.7  $\pm$  0.4 kcal mol<sup>-1</sup> has been reported by Dombrowski et al.<sup>11</sup>, and a BDE(R–H) = 91.2  $\pm$  2 kcal mol<sup>-1</sup> has been reported by Wayner et al.<sup>10</sup> <sup>j</sup> Tetrahydrofuran, neat liquid. A correction of -1 kcal mol<sup>-1</sup> in  $\Delta_6 H_{\text{obs}}$  and  $\Delta_9 H_{\text{obs}}$  is included for the contribution of  $\beta$ -hydrogen abstraction.<sup>5c</sup> <sup>k</sup> Dioxane, competition experiments with different concentrations of CHD (0.2–0.5 M), see eq 13. The BDE(R–OO) has been determined by a competition experiment with 0.3 M CHD and 11.4 M dioxane. With  $\Delta_9 H_{\text{obs}} = -52$  kcal mol<sup>-1</sup>,  $\Delta_9 H_{\text{obs,CHD}} = -51$  kcal mol<sup>-1</sup>, and  $\xi = 0.39$ ,  $\Delta_9 H_{\text{obs,DIOX}}$  becomes -54 kcal mol<sup>-1</sup>.

of a photochemical active complex. As the calibration is performed under the same conditions (solvent composition), this additional enthalpic contribution does not effect the  $\Delta_9 H_{\text{obs}}$ .

From the difference between  $\Delta_9 H_{\text{obs}}$  and  $\Delta_6 H_{\text{obs}}$ , the BDE(R–OO) can be retrieved according to eq 10:

$$\text{BDE(R–OO)} = -0.5(\Delta_9 H_{\text{obs}} - \Delta_6 H_{\text{obs}}) - \Delta V_4/\chi_s \quad (10)$$

The magnitude of the chemical volume change ( $\Delta V_4/\chi_s$ ) in eq 4 has been determined to be  $4.0 \pm 0.3$  kcal mol<sup>-1</sup> for various solvents.<sup>5a</sup> Considering that the difference in number of species on going from reactants to products in eq 1 is equal but opposite in sign, it is reasonable to assume that  $\Delta V_4/\chi_s = -\Delta V_1/\chi_s$ .<sup>4</sup>

Thus, the BDE(R–H) and BDE(R–OO) for cyclohexane (CHEX), 1,4-cyclohexadiene (CHD), pyrrolidine (PYR), triethylamine (TEA), tetrahydrofuran (THF), and 1,4-dioxane (DIOX) have been determined (see Table 1).

The time window for PAC is around 300 ns in which all the heat needs to be deposited into the solution.<sup>5c</sup> In the case of CHEX and DIOX, the hydrogen abstraction reaction (eq 5) is too slow even with the neat liquids. To reduce the lifetime of the *tert*-butoxyl radicals, a second reagent (1,4-cyclohexadiene) from which a hydrogen can be abstracted is added to the liquid A. The observed enthalpy is now a combination of the two competing hydrogen atom abstraction reactions. Provided that the rate constants for eq 5 are available (vide infra), the reaction

enthalpy for compound A can be retrieved using eqs 11 and 12.

$$\Delta_6 H_{\text{obs}} = \xi \Delta_6 H_{\text{obs,A}} + (1 - \xi) \Delta_6 H_{\text{obs,CHD}} \quad (11)$$

$$\xi = \frac{k_{5,A}[A]}{k_{5,A}[A] + k_{5,\text{CHD}}[\text{CHD}]} \quad (12)$$

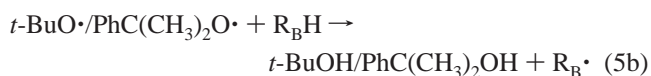
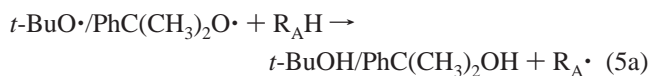
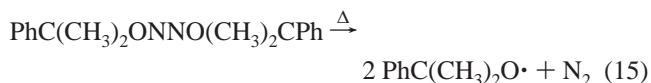
When a series of concentrations is used, it is convenient to rearrange eq 11 into eq 13:

$$\Delta_6 H_{\text{obs}} = \Delta_6 H_{\text{obs,CHD}} + \xi(\Delta_6 H_{\text{obs,A}} - \Delta_6 H_{\text{obs,CHD}}) \quad (13)$$

A plot of  $\Delta_6 H_{\text{obs}}$  vs  $\xi$  according to eq 13, with four different concentrations of CHD (0.2–0.5 M,  $\xi = 0.26-0.50$ ) in DIOX, resulted in a straight line ( $r^2 = 0.97$ ) with slope ( $\Delta_6 H_{\text{obs,A}} - \Delta_6 H_{\text{obs,CHD}}$ ) = 41 kcal mol<sup>-1</sup> and intercept ( $\Delta_6 H_{\text{obs,CHD}}$ ) = -34 kcal mol<sup>-1</sup>, and hence,  $\Delta_6 H_{\text{obs,DIOX}} = 7$  kcal mol<sup>-1</sup>. The intercept,  $\Delta_6 H_{\text{obs,CHD}} = -34$  kcal mol<sup>-1</sup>, is close to the value obtained with CHD in ethyl acetate (see Table 1).

Upon saturation with oxygen,  $\xi$  does not change since all radicals will be quantitatively trapped.

**Rate Constants for Hydrogen Abstraction ( $k_5$ ).** Hydrogen atom abstraction rate constants by *tert*-butoxyl,  $k_5$ , for CHEX and DIOX as measured by Laser Flash Photolysis (LFP) cannot be used in this study. It has been found that for THF the LFP determined rate constant (obtained in dilute solutions) differs markedly (around a factor of 2 higher) from the one derived from PAC competition experiments (see eqs 11 and 12) at high substrate concentration.<sup>5c</sup> To obtain  $k_5$  values applicable to the PAC conditions, we have conducted a number of product studies in sealed tubes with mixtures of reagents (without any solvent) at two different temperatures. Thermolysis of di-*tert*-butylperoxide at 393 K (eq 14) or dicumylhyponitrite at 318 K (eq 15) was used to generate *tert*-butoxyl radicals or cumylxoyl radicals, respectively.<sup>12</sup> After hydrogen atom abstraction (eqs 5a and 5b) by the alkoxyl radical and in the presence of TEMPO (T) as the radical trap, two stable N-alkoxylamines (R<sub>A</sub>-T and R<sub>B</sub>-T) are formed (eqs 16a and 16b). ).



Provided that all carbon-centered radicals are scavenged with the same efficiency, the product ratio [R<sub>A</sub>-T]/[R<sub>B</sub>-T] can be used to derive to rate constant ratio for hydrogen atom abstraction: [R<sub>A</sub>-T]/[R<sub>B</sub>-T] =  $k_{5,a}/k_{5,b}[\text{R}_A\text{H}]/[\text{R}_B\text{H}]$ .

With various mixtures of DIOX and THF, a  $k_{5,\text{THF}}/k_{5,\text{DIOX}}$  of 4.1 was obtained at 393 K. Accepting the same preexponential factors on a per-H basis,  $k_{5,\text{THF}}/k_{5,\text{DIOX}} = 8.4$  at 298 K. The absolute rate constant for hydrogen atom abstraction from THF is known,  $k_{5,\text{THF}} = 4.4 \times 10^6$  M<sup>-1</sup> s<sup>-1</sup>,<sup>5c</sup> thus,  $k_{5,\text{DIOX}} = 5.3 \times$

**TABLE 2: BDE(R–H) and BDE(R–OO) (kcal mol<sup>-1</sup>) at 298 K Determined by Density Functional Theory [B3LYP/6-31G(d)//B3LYP/6-31G(d)] and by Experimental Methods**

R	DFT		experimental	
	BDE(R–H) <sup>a</sup>	BDE(R–OO) <sup>a</sup>	BDE(R–H) <sup>b</sup>	BDE(R–OO)
1, CH <sub>3</sub>	105.0 (105.7)	31.4(31.1)	105	33 <sup>c</sup>
2, C <sub>2</sub> H <sub>5</sub>	100.3 (101.0)	32.4	101	35 <sup>c</sup>
3, C <sub>3</sub> H <sub>7</sub>	100.9 (101.6)	33.0	101	
4, CH <sub>3</sub> CHCH <sub>3</sub>	96.4 (97.1)	32.3	98	37 <sup>c</sup>
5, C(CH <sub>3</sub> ) <sub>3</sub>	93.2 (94.0)	31.4(31.4)	96	37 <sup>c</sup>
6, <i>c</i> -C <sub>3</sub> H <sub>5</sub>	106.4 (107.2)	39.5		
7, <i>c</i> -C <sub>4</sub> H <sub>7</sub>	97.3 (98.0)	34.2		
8, <i>c</i> -C <sub>6</sub> H <sub>11</sub>	96.9 (97.6)	32.7	97 <sup>d</sup>	24 <sup>d,e</sup>
9, C <sub>2</sub> H <sub>3</sub>	109.3	45.2	111	
10, CH <sub>2</sub> =CCH <sub>3</sub> <sup>f</sup>	105.7	44.1		
11, C <sub>6</sub> H <sub>5</sub>	110.8	46.2	113	
12, CH <sub>2</sub> =CHCH <sub>2</sub>	85.0 (85.9)	14.8	88	18 <sup>c</sup>
13, CH <sub>2</sub> =CHCHCH <sub>3</sub>	80.2 (81.5)	14.9	84	
14, <i>c</i> -C <sub>6</sub> H <sub>7</sub> <sup>g</sup>	71.4 (72.3)	5.9	77 <sup>d</sup>	12 <sup>d</sup>
15, C <sub>6</sub> H <sub>5</sub> CH <sub>2</sub>	87.8 (88.6)	18.2	90	22 <sup>c</sup>
16, C <sub>6</sub> H <sub>5</sub> CHCH <sub>3</sub>	84.8 (85.7)	18.9	87	
17, <i>c</i> -C <sub>4</sub> H <sub>8</sub> N	88.2	27.8	87 <sup>d</sup>	10 <sup>d,e</sup>
18, (C <sub>2</sub> H <sub>5</sub> ) <sub>2</sub> NCHCH <sub>3</sub>	89.9 <sup>h</sup>	30.2	89 <sup>d</sup>	25 <sup>d,e</sup>
19, C <sub>4</sub> H <sub>7</sub> O	90.7 (91.6) <sup>i</sup>	32.4	92 <sup>d</sup>	32 <sup>d</sup>
20, C <sub>4</sub> H <sub>7</sub> O <sub>2</sub>	94.6	31.6	96 <sup>d</sup>	34 <sup>d</sup>
21, CCl <sub>3</sub>	92.1	17.2	96	20 <sup>c</sup>

<sup>a</sup> BDEs in parentheses are calculated on the B3LYP/6-31(d,p) level.<sup>16</sup> <sup>b</sup> Recommended literature values, ref 16 and references therein and ref 17. <sup>c</sup> References 18 (compounds 1, 2, 4, 5, and 21), 19 (12), and 20 (15). <sup>d</sup> This work. <sup>e</sup> This value does not refer to the BDE(R–OO); see text.<sup>f</sup> The carbon centered radical used for the calculation was marked as a transition state. Attempts to find the global minimum were not successful. <sup>g</sup> If the spin density distribution in cyclohexadienyl determines the product ratio of *c*-C<sub>6</sub>H<sub>7</sub> + O<sub>2</sub>, then 60% 1,3-CHD peroxy and 40% 1,4-CHD peroxy are formed. The BDE(R–OO) for both compounds differ by only 0.1 kcal mol<sup>-1</sup>. DFT calculates a bond length of 1.4799 and 1.5033 Å for 1,3-CHD-OO and 1,4-CHD-OO, respectively. <sup>h</sup> No optimal geometry could be calculated by DFT. A geometry with a deviation of 8% above the maximum force parameter was used to calculate the vibrational energies. <sup>i</sup> References 4 and 16.

10<sup>5</sup> M<sup>-1</sup> s<sup>-1</sup>. Analogously, with mixtures of DIOX and CHEX,  $k_{5,\text{CHEX}}/k_{5,\text{DIOX}}$  was found to be 1.2 at 393 K, leading to  $k_{5,\text{CHEX}} = 6.2 \times 10^5 \text{ M}^{-1} \text{ s}^{-1}$  at 298 K.

At 318 K, and with dicumylhyponitrite as the source for alkoxy radicals,  $k_{5,\text{THF}}/k_{5,\text{DIOX}} = 7.6$  and  $k_{5,\text{CHEX}}/k_{5,\text{DIOX}} = 1.4$ , to give  $k_{5,\text{DIOX}} = 4.9 \times 10^5 \text{ M}^{-1} \text{ s}^{-1}$  and  $k_{5,\text{CHEX}} = 6.6 \times 10^5 \text{ M}^{-1} \text{ s}^{-1}$  at 298 K.<sup>13</sup>

The average of both sets of experiments leads to the following absolute rate constants at 298 K:  $k_{5,\text{DIOX}} = 5.1 \times 10^5 \text{ M}^{-1} \text{ s}^{-1}$  and  $k_{5,\text{CHEX}} = 6.4 \times 10^5 \text{ M}^{-1} \text{ s}^{-1}$ . The obtained ratio of  $k_{5,\text{DIOX}}:k_{5,\text{CHEX}}:k_{5,\text{THF}}$  of 1:1.3:6.9 is remarkably close to the one which can be derived from the LFP data (1:1.1:5.5) while the absolute values differ:  $k_{5,\text{DIOX}} = 1.5 \times 10^6$ ,  $k_{5,\text{CHEX}} = 1.6 \times 10^6$ , and  $k_{5,\text{THF}} = 8.25 \times 10^6 \text{ M}^{-1} \text{ s}^{-1}$ .<sup>14</sup>

**Effect of Solvation.** To allow a comparison of the PAC data with enthalpic information retrieved from gas-phase experiments and theoretical computations, solvation effects on the heat of eq 1 need to be taken into consideration. The heat of solvation for molecular oxygen in (a)polar organic solvents is less than 0.5 kcal mol<sup>-1</sup>.<sup>15</sup> The contribution to the  $\Delta H_{\text{obs}}$  can be considered negligible in view of the experimental uncertainties ( $\pm 1$ –1.5 kcal mol<sup>-1</sup>). Therefore, only the difference in solvation enthalpy between the peroxy radical and the carbon-centered radical may influence the overall enthalpy balance. To quantify this solvent effect, experiments with 1,4-cyclohexadiene have been repeated in a polar solvent, ethyl acetate, to yield  $\Delta_9 H_{\text{obs}} = -51 \text{ kcal mol}^{-1}$ . The difference with the  $-45 \text{ kcal mol}^{-1}$  in isooctane consists of an additional solvation enthalpy of 4 kcal mol<sup>-1</sup> due to the *t*-BuOH/*t*-BuOOBu-*t* couple, and hence, the remaining 2 kcal mol<sup>-1</sup> can be associated with twice the difference in solvation enthalpy due to the alkyl radical/peroxy couple. This is well outside the error margin. Thus, in ethyl acetate a BDE(R–OO) of 13 kcal mol<sup>-1</sup> has been obtained as opposed to 12 kcal mol<sup>-1</sup> obtained in isooctane. The small but significant difference provides an assessment of the change in

the heat of solvation in polar solvents. The correction of 2 kcal mol<sup>-1</sup> has been applied to remove the solvation contribution in the  $\Delta_9 H_{\text{obs}}$  for tetrahydrofuryl-O<sub>2</sub> and dioxanyl-O<sub>2</sub>, since THF, DIOX, and ethyl acetate have similar polarities.

The PAC heat of reaction for triethylamine did not change from isooctane to ethyl acetate.

**DFT Reaction Enthalpy for R• + O<sub>2</sub> → R–OO•.** The calculated BDE(R–H) and BDE(R–OO) at 298 K on the B3LYP/6-31G(d) level for a range of compounds, including the ones determined experimentally, are given in Table 2 and refer to the lowest energy conformers for RH, R•, and R–OO•.

Also included are BDE(R–H)s from computational studies using the 6-31G(d,p) basis set.<sup>16</sup> In general, these results are around 1 kcal mol<sup>-1</sup> higher. From Table 2, it can be inferred that DFT at the 6-31G(d) level underestimates the BDE(R–H) for hydrocarbons and compounds containing heteroelements by 0–3 kcal mol<sup>-1</sup> with respect to (evaluated) experimental values. A clear exception is 1,4-cyclohexadiene for which the deviation amounts to 5–6 kcal mol<sup>-1</sup> with both basis sets. An erroneous handling of multiple unsaturated moieties in the closed shell molecule seems to be the main source of error.<sup>16</sup> To evaluate if the application of a higher basis set is beneficial for the BDE(R–OO) computations, the calculations for methyl and *tert*-butyl have been repeated employing the 6-31G(d,p) basis set. The differences with the less time-consuming 6-31G(d) appeared to be less than 0.3 kcal mol<sup>-1</sup> (see Table 2).

Our results show that DFT underestimates the absolute BDE(R–OO) by 0–6 kcal mol<sup>-1</sup>. As has been found before<sup>21</sup> for BDE(C–O), BDE(O–H), and BDE(O–O), DFT on the 6-31G(d) or 6-31G(d,p) level systematically predicts lower values (by 3–6 kcal mol<sup>-1</sup>) for bonds involving the element oxygen.

To eliminate any deviation originating from the computation of the carbon skeleton, the differences between BDE(R–OO) and BDE(R–H), i.e., the heat of reaction for the reaction of  $\text{RH} + \text{O}_2 \rightarrow \text{R–OO}\cdot + \text{H}\cdot$ , have been compiled in Table 3.

**TABLE 3: Difference between BDE(R–H) and BDE(R–OO) (kcal mol<sup>-1</sup>)<sup>a</sup> and Entropy for the Reaction 1 R· + O<sub>2</sub> → ROO· (cal mol<sup>-1</sup> K<sup>-1</sup>)<sup>b</sup>**

R	ΔBDE		Δ <sub>1</sub> S <sup>o</sup>	
	DFT	exp <sup>c</sup>	DFT	exp <sup>c</sup>
1, CH <sub>3</sub>	73.6	72	-35	-31
2, C <sub>2</sub> H <sub>5</sub>	67.9	66	-40	-34
3, C <sub>3</sub> H <sub>7</sub>	67.9		-42	
4, CH <sub>3</sub> CHCH <sub>3</sub>	64.1	61	-43	-37
5, C(CH <sub>3</sub> ) <sub>3</sub>	61.8	59	-43	-40
6, <i>c</i> -C <sub>3</sub> H <sub>5</sub>	66.9		-38	
7, <i>c</i> -C <sub>4</sub> H <sub>7</sub>	63.1		-42	
8, <i>c</i> -C <sub>6</sub> H <sub>11</sub>	64.2		-40	
9, C <sub>2</sub> H <sub>3</sub>	64.1		-37	
10, CH <sub>2</sub> =CCH <sub>3</sub>	61.6		-35	
11, C <sub>6</sub> H <sub>5</sub>	64.6		-38	
12, CH <sub>2</sub> =CHCH <sub>2</sub>	70.2	70	-37	-31
13, CH <sub>2</sub> =CHCHCH <sub>3</sub>	65.3		-38	
14, <i>c</i> -C <sub>6</sub> H <sub>7</sub>	65.5	65	-36	
15, C <sub>6</sub> H <sub>5</sub> CH <sub>2</sub>	69.6	68	-35	-34
16, C <sub>6</sub> H <sub>5</sub> CHCH <sub>3</sub>	65.9		-39	
17, C <sub>4</sub> H <sub>8</sub> N	60.4		-35	
18, (C <sub>2</sub> H <sub>5</sub> ) <sub>2</sub> NCHCH <sub>3</sub>	59.7		-38	
19, C <sub>4</sub> H <sub>7</sub> O	58.3	60	-38	
20, C <sub>4</sub> H <sub>7</sub> O <sub>2</sub>	63.0	62	-38	
21, CCl <sub>3</sub>	74.9	76	-38	-40

<sup>a</sup> Absolute values: see Tables 1 and 2. <sup>b</sup> Calculated [at B3LYP/6-31G(d)//B3LYP/6-31G(d) level] and experimental values. <sup>c</sup> References 18 (**1**, **2**, **4**, **5**, and **21**), 19 (**12**), and 20 (**15**).

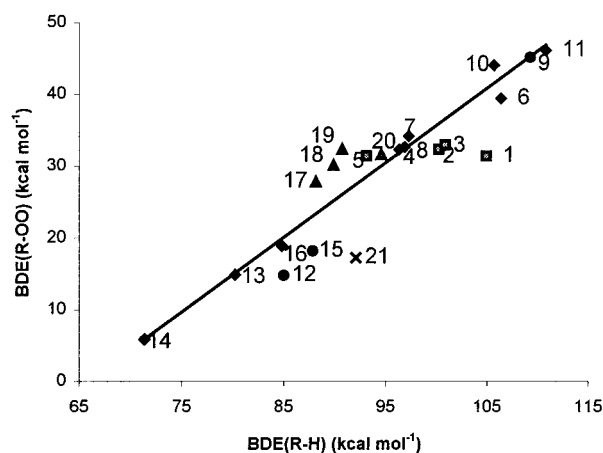
Indeed, the agreement between computational and experimental enthalpic data is now greatly improved.

**DFT Substituent Effect on BDE(R–OO).** From Table 2, it is obvious that the BDE(R–OO) is almost invariant when oxygen is attached to (a)cyclic saturated hydrocarbons. Thus, from methyl to *tert*-butyl, the BDE(R–H) decreases by 12 kcal mol<sup>-1</sup> while the BDE(R–OO) remains almost constant. An anomaly is cyclopropane caused by the olefinic nature of the carbon atoms in the ring. Similarly, no effect on the BDE(R–OO) by methyl substitution is found for vinylic, allylic, and benzylic compounds. From experimental thermodynamic data, it can be inferred that this “no next nearest neighbor contribution”<sup>22</sup> also holds for bonds between carbon and electronegative groups such as OH and Cl.<sup>23</sup> Thus, the stabilization enthalpies for the closed shell molecule and the radical are similar. A rationale for this phenomenon may be the occurrence of an additional electronic (lone pair) interaction in the ground state.

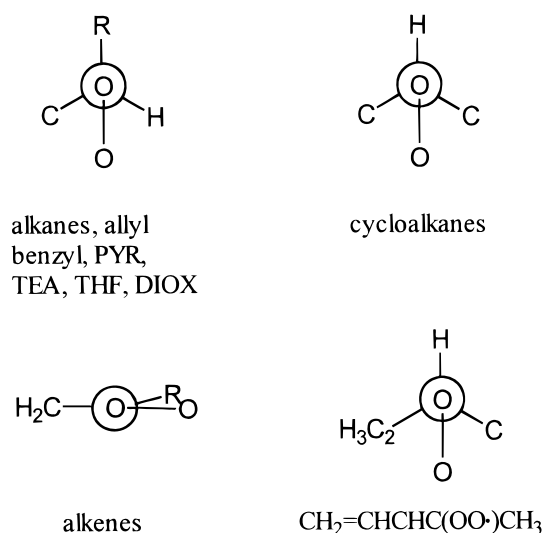
A plot of the DFT BDE(R–OO) versus the BDE(R–H), for hydrocarbons with a linkage between a secondary carbon and oxygen (irrespective of the hybridization), shows a perfect linear correlation: BDE(R–OO) = 1.04 BDE(R–H) – 68.4 with  $r^2 = 0.99$  (see Figure 1). The slope of almost unity indicates that the change in (Pauling’s) electronegativity between the R–OO and the R–H bonds remains virtually constant. Similar correlation’s can be obtained for primary or tertiary carbon–hydrogen/carbon–oxygen bonds as the one displayed in Figure 1 but with a slightly different intercept.

Figure 1 shows that when a heteroelement (oxygen or nitrogen) is attached to the α-carbon as in PYR, TEA, or THF, the BDE(R–OO)s are relatively stronger, but on the other hand, DIOX follows the hydrocarbon behavior.

**DFT Reaction Entropy for R· + O<sub>2</sub> → R–OO·.** The reaction entropies for eq 1, Δ<sub>1</sub>S, are presented in Table 3. In general, DFT predicts a somewhat higher loss in entropy compared to other studies. However, it should be noticed that in most cases the reported “experimental” ΔS values are actually derived by group additivity methods or by ab initio calculations.



**Figure 1.** Relation between BDE(R–OO) and BDE(R–H) (kcal mol<sup>-1</sup>) calculated by DFT. BDE(R–OO) = 1.04BDE(R–H) – 68.4 for secondary hydrocarbons (♦). Compounds are listed in Table 2.



**Figure 2.** Newman projections of the lowest enthalpy conformations of R–OO·.

In any case, when calculating the ΔH from an equilibrium constant for eq 1, a difference of 3 cal mol<sup>-1</sup> K<sup>-1</sup> (for *tert*-butyl, see Table 3) renders a minor change of 0.89 kcal mol<sup>-1</sup> in the BDE(R–OO).

**DFT Conformers, Spin Densities, and Charge Distributions for ROO·.** The geometry optimizations reveal a particular lowest energy conformation for each class of compounds. Newman projections are displayed in Figure 2.

For ethyl, *n*-propyl-, and *i*-propyl peroxy, the second oxygen prefers a position gauche to the α-hydrogen and the α-methyl group. A conformation for oxygen gauche to two α-hydrogens (ethyl, *n*-propyl peroxy) or to two α-methyls (*i*-propyl peroxy) is recognized as a transition state. The same conformation is found for PYR, TEA, and THF peroxy: the second oxygen is almost anti to the nitrogen or oxygen of the parent compound. For DIOX, the first oxygen is in the axial position and the second oxygen is anti to the oxygen in the ring. In the cycloalkanes, the terminal oxygen is pointing toward the ring and the axial cyclohexyl-O<sub>2</sub> conformer is lowest in energy. If the O<sub>2</sub> is attached to an sp<sup>2</sup> carbon (compounds **9**, **10**, and **11**), the second oxygen is in the same plane as the C=C–O, and in the case of **9** and **10**, it is directed away from the double bond. For the allylic and benzylic lowest energy conformations, the second oxygen is gauche to the α-hydrogen and the α-vinyl or α-phenyl groups. The only exception is the lowest energy

conformer of  $\text{CH}_2=\text{CHCH}(\text{OO}\cdot)\text{CH}_3$ : the second oxygen prefers a position *gauche* relative to methyl and vinyl.<sup>24</sup>

DFT calculated a spin distribution for the peroxy radical of 70% on the terminal oxygen and 30% on the oxygen attached to carbon for all compounds investigated.

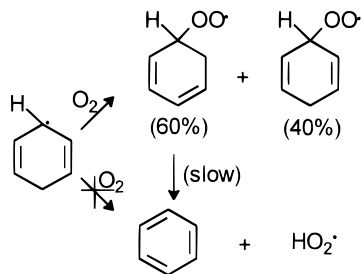
The Mulliken charges (with hydrogen atoms summed into the heavy atoms) on  $\alpha$ -carbon are between +0.28 and +0.32 for alkanes and cycloalkanes, +0.35 for olefines and benzene, and +0.20 for allylic and benzylic compounds. For PYR, TEA, THF, and DIOX, the charges are notably higher: +0.43, +0.39, +0.50, and +0.52, respectively, caused by the presence of the electronegative element attached to the  $\alpha$ -carbon. The Mulliken charges on the first oxygen are almost constant, -0.16 to -0.19. Exceptions are the phenylperoxy and the trichloromethylperoxy with charges on oxygen of -0.24 and -0.11, respectively.

## Discussion

Dynamic studies by laser flash photolysis in the liquid phase have demonstrated that rate constants for the reaction of carbon-centered radicals with molecular oxygen are near or at the diffusion limit, and they merely reflect the transport behavior in the medium. No information can be retrieved as to the followed reaction pathways: recombination *and/or* disproportionation.<sup>25</sup> On the contrary, the enthalpic effect measured by photoacoustic calorimetry represents the chemical change immediately after the encounter of the two species. When recombination (eq 1) is the sole pathway, the BDE(R-OO) can be retrieved directly from the observed reaction enthalpy. On the other hand, an obvious discrepancy between the results obtained by PAC and by other methods (e.g., DFT) is indicative for the presence of other processes such as disproportionation.

**Cyclohexyl + O<sub>2</sub> and Cyclohexadienyl + O<sub>2</sub>.** It has been frequently suggested that under oxidative conditions disproportionation is the only reaction channel for cyclohexadienyl radicals because benzene is obtained as the main reaction product.<sup>26</sup> The enthalpy change for this reaction (eq 3) can be estimated to be  $-28 \text{ kcal mol}^{-1}$ ,<sup>23</sup> which deviates substantially from the experiment.<sup>27</sup> Hence, recombination is the only (major) pathway. A pulse radiolysis study in water has shown that oxygen is exclusively adding to the cyclohexadienyl radical, to yield a mixture of 1,3- and 1,4-cyclohexadienyl peroxy species in a ratio of 60 and 40% respectively, in accordance with the spin densities calculated by DFT (see Table 2).<sup>28</sup> Subsequent decay, with a global rate constant of ca.  $8 \times 10^5 \text{ s}^{-1}$ ,<sup>28</sup> yields, in part, benzene and HO<sub>2</sub><sup>•</sup> (see Scheme 1).

### SCHEME 1



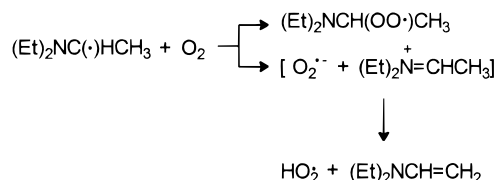
In view of the short time window for PAC, the secondary reaction enthalpies will not be part of the integrated heat. In another pulse radiolysis study a BDE(R-OO) of  $5.5 \text{ kcal mol}^{-1}$  was derived, at variance by  $6 \text{ kcal mol}^{-1}$  with the present results. As already indicated in that report, due to the complexity of the kinetic model used, thermodynamic conclusions seem to be unpromising.<sup>29</sup> Furthermore, the heat of solvation for oxygen

in water of  $-2.9 \text{ kcal mol}^{-1}$ <sup>30</sup> has not been incorporated, and the heat of solvation for the organic peroxy radical is likely to be different in water compared to organic solvents.

In view of the large difference found by PAC with mixtures of CHEX and CHD or CHEX and THF (see Table 1), we are unable to determine the BDE(R-OO) by this method due to unknown reasons.

**1-(Diethylamino)ethyl + O<sub>2</sub> and 1-Pyrrolidinyl + O<sub>2</sub>.** The obtained BDE(R-OO) for 1-(diethylamino)ethyl peroxy radical of  $25 \text{ kcal mol}^{-1}$  is clearly too low compared to the DFT computed value of ca.  $30 \text{ kcal mol}^{-1}$ . This indicates the presence of an additional reaction pathway for the  $\alpha$ -aminoalkyl radical and oxygen. It is known that the autoxidation of triethylamine in hydrocarbon solvents involves the hydroperoxy radical rather than the organic peroxy radical as the chain carrier.<sup>31</sup> In water, after hydrogen atom abstraction from trimethylamine, the (dimethylamino)methyl radical is oxidized by oxygen to yield the superoxide anion ( $\text{O}_2^{\bullet-}$ ) and the dimethyliminium ion<sup>32</sup> either by electron transfer via a short-lived organic peroxy radical or by direct electron transfer. In aqueous media, the latter pathway is probably more favored for the 1-(diethylamino)ethyl radical because the oxidation potential is lower ( $E_{\text{ox}}$  is  $-1.36$  and  $-1.27 \text{ V}$  vs NHE, respectively).<sup>33</sup> However, it seems unlikely that the formation an ion pair or separate ionic species is feasible in organic solvents due to the diminished stabilization by solvation. Indeed, the observed reaction enthalpy is not affected by changing the polarity of the solvent (isooctane vs ethyl acetate), which seems to exclude any ionic intermediates. Thus, disproportionation may take place through electron transfer followed by proton transfer in the early stage of reaction, and the formal disproportionation products, diethylvinylamine and the hydroperoxy radical, are obtained (see Scheme 2). Comparing estimated reaction enthalpies for the 1-(diethylamino)ethyl radical (eqs 1 and 3) with the experimental data<sup>34</sup> shows that competition may exist between recombination and disproportionation, with recombination as the major reaction pathway.

### SCHEME 2



The oxidation potential for 1-pyrrolidinyl radical is expected to be even lower. Surprisingly, for the 1-pyrrolidinyl radical, the estimated reaction enthalpy for disproportionation<sup>35</sup> is close to the experimental value. The observations are still suggestive for an ionic component in the oxidation of  $\alpha$ -aminoalkyl radicals.

**Tetrahydrofuryl + O<sub>2</sub> and Dioxanyl + O<sub>2</sub>.** The increase in BDE(R-H) from CHD to THF is  $15 \text{ kcal mol}^{-1}$ , while for the BDE(R-OO), the difference is  $20 \text{ kcal mol}^{-1}$ . Hence, the BDE(R-OO) in THF is stronger by  $5 \text{ kcal mol}^{-1}$ . A smaller effect can be noticed for DIOX. DFT calculated values show a similar trend.

The spin density on the  $\alpha$ -carbon is lower than unity, due to the interaction with the lone pair of oxygen, the BDE(R-H) in, e.g., THF is lowered. The positive charge on carbon in the peroxy radical is significantly higher compared with hydrocarbons. As a result, the C-O bond is stronger due to an increase in polar contribution. However, no correlation can be

found between the polarity of the C–O bond (product of the charges on carbon and oxygen) and the BDE(R–OO).

Although the bonds are more polarized, the R–OO bonds in THF and DIOX are longer relative to the R–OO bonds (as shown by DFT) in secondary alkanes as predicted by anomeric interactions. The interaction of the oxygen lone pair with the  $\sigma^*$  carbon–OO bonding orbital renders an additional contribution to the heat of formation of the peroxyl radical. For DIOX, this stabilizing interaction is reduced due to conformational restraints.<sup>4</sup>

**Acknowledgment.** The authors thank Keith Ingold (Stacie Institute Molecular Sciences, NRC, Canada) for kindly supplying a sample of sodiumhyponitrite, Mats Jonsson (Royal Institute of Technology, Stockholm, Sweden), and Dan Wayner (NRC, Canada) for the stimulating discussion. One of us (A.C.) thanks the Wenner-Gren Foundation for financial support.

## References and Notes

- (1) (a) Maillard, B.; Ingold, K. U.; Scaiano, J. C. *J. Am. Chem. Soc.* **1983**, *105*, 5095. (b) Neta, P.; Grodkowski, J.; Ross, A. B. *J. Phys. Chem. Ref. Data* **1996**, *25*, 709.
- (2) Ignatyev, I. S.; Xie, Y.; Allen, W. D.; Schaefer, H. F. *J. Chem. Phys.* **1997**, *107*, 141.
- (3) Knyazev, V. D.; Slagle, I. R. *J. Phys. Chem. A* **1998**, *102*, 1770.
- (4) Ciriano, M. V.; Korth, H.-G.; Van Scheppingen, W. B.; Mulder, P. *J. Am. Chem. Soc.* **1999**, *121*, 6375–6381.
- (5) (a) Wayner, D. D. M.; Luszyk, E.; Pagé, O.; Ingold, K. U.; Mulder, P.; Laarhoven, L. J. J.; Aldrich, H. S. *J. Am. Chem. Soc.* **1995**, *117*, 8737. (b) Laarhoven, L. J. J.; Mulder, P.; Wayner, D. D. M. *Acc. Chem. Res.* **1999**, *32*, 342. (c) Laarhoven, L. J. J.; Mulder, P. *J. Phys. Chem.* **1997**, *101*, 73.
- (6) Dulog, L.; Klein, P. *Chem. Ber.* **1971**, *104*, 895.
- (7) Scott, A. P.; Radom, L. *J. Phys. Chem.* **1996**, *100*, 16502.
- (8) For the applied solvents, the oxygen concentrations at upon saturation 298 K are cyclohexane,  $1.1 \times 10^{-2}$  M; ethyl acetate,  $1.1 \times 10^{-2}$  M; isooctane,  $1.5 \times 10^{-2}$  M; dioxane,  $6.3 \times 10^{-3}$  M; tetrahydrofuran,  $1.0 \times 10^{-2}$  M.<sup>9</sup>
- (9) (a) Battino, R. (Ed.) *IUPAC Solubility data series*; Pergamon Press: Oxford, 1981; Vol. VII, p 301. (b) Murov, S. L. *Handbook of photochemistry*; Marcel Dekker: New York, 1973; p 89.
- (10) Wayner, D. D. M.; Clark, K. B.; Rauk, A.; Yu, D.; Armstrong, D. A. *J. Am. Chem. Soc.* **1997**, *119*, 8925.
- (11) Dombrowski, G. W.; Dinnoncenco, J. P.; Farid, S.; Goodman, J. L.; Gould, I. R. *J. Org. Chem.* **1999**, *64*, 427.
- (12) The reactivity of *tert*-butoxyl and cumyloxyl radicals are comparable. Baignée, A.; Howard, J. A.; Scaiano, J. C.; Stewart, L. C. *J. Am. Chem. Soc.* **1983**, *105*, 6120.
- (13) Relative to *tert*-butyl alcohol (yield 74%), the total yield of R–T products is 60% in the experiment with THF and DIOX and 67% for a mixture of CHEX and DIOX. Not all *t*-BuOOBu-*t* was converted during the experiment. Relative to cumyl alcohol (yield 85%), the total yield of R–T is 77% in the experiment with THF and DIOX and 96% for a mixture of CHEX and DIOX. It is assumed that radical coupling (R• + TEMPO) is the sole reaction pathway (only traces of TEMPO-H were found). All methyl radicals formed in the unimolecular decomposition of the alkoxy radicals are trapped by the excess TEMPO. Only small amounts of CH<sub>3</sub>•T are obtained.
- (14) Malatesta, V.; Scaiano, J. C. *J. Org. Chem.* **1982**, *47*, 1455.
- (15) Wilhelm, E.; Battino, R. *Chem. Rev.* **1973**, *73*, 1.
- (16) Santoro, D.; Korth, H.-G.; Mulder, P. *J. Chem. Soc., Perkin Trans 2* (submitted for publication).
- (17) Tsang, W. in *Energetics of organic free radicals*; Simões, J. A. M., Greenberg, A., Liebman, J. F., Eds.; Blackie Academic & Professional: Glasgow, 1996; p 54.
- (18) Knyazev, V. D.; Slagle, I. R. *J. Phys. Chem. A* **1998**, *102*, 1770.
- (19) Morgan, C. A.; Pilling, M. J.; Tulloch, J. M.; Ruiz, R. P.; Bayes, K. D. *J. Chem. Soc., Faraday Trans. 2* **1982**, *78*, 1323.
- (20) Fenter, F. F.; Nozière, B.; Caralp, F.; Lesclaux, R. *Int. J. Chem. Kin.* **1994**, *26*, 171.
- (21) Van Scheppingen, W. B.; Dorrestijn, E.; Arends, I. W. C. E.; Mulder, P.; Korth, H.-G. *J. Phys. Chem. A* **1997**, *101*, 5404.
- (22) Slagle, I. R.; Ratajczak, E.; Heaven, M. C.; Gutman D.; Wagner, A. F. *J. Am. Chem. Soc.* **1985**, *107*, 1838.
- (23) (a) *NIST Chemistry WebBook*; Mallard, W. G., Ed.; NIST Standard Reference Database 69–November 1998 Release, National Institute of Standards and Technology: Gaithersburg, MD, 1998. (b) Stein, S. E.; Rukkers, J. M.; Brown, R. L. *NIST Structures and Properties Database*, version 2.0; NIST Standard Reference Data; National Institute of Standards and Technology: Gaithersburg, MD, 1994.
- (24) The conformer with the second oxygen gauche to the  $\alpha$ -hydrogen and the  $\alpha$ -methyl is marked as a transition state.
- (25) Arends, I. W. C. E.; Mulder, P.; Clark, K. B.; Wayner, D. D. M. *J. Phys. Chem.* **1995**, *99*, 8182.
- (26) Hendry, D. G.; Schuetzle, D. *J. Am. Chem. Soc.* **1975**, *97*, 7123.
- (27) For eq 3, no volume correction is required (see eq 10), hence  $\Delta_9H_{\text{obs}} - \Delta_6H_{\text{obs}}$  represents twice the heat for eq 3. For cyclohexadienyl a value of  $-56 \text{ kcal mol}^{-1}$  would have been expected, while experimentally  $-16 \text{ kcal mol}^{-1}$  has been obtained.
- (28) Pan, X.-M.; Schuchmann, M. N.; von Sonntag, C. *J. Chem. Soc., Perkin Trans 2* **1993**, 1021.
- (29) Fang, X.; Pan, X.; Rahmann, A.; Schuchmann, H.-P.; von Sonntag, C. *Chem. Eur. J.* **1995**, *1* (7), 423.
- (30) Wilhelm, E.; Battino, R.; Wilcock, R. *J. Chem. Rev.* **1977**, *77*, 219.
- (31) Howard, J. A.; Yamada, T. *J. Am. Chem. Soc.* **1981**, *103*, 7102.
- (32) Von Sonntag, C.; Schuchmann, H.-P. *Angew. Chem., Int. Ed. Engl.* **1991**, *20*, 1229.
- (33) Jonsson, M.; Kraatz, H.-B. *J. Chem. Soc., Perkin Trans 2* **1997**, 2673.
- (34) Assuming that only eq 3 is operative,  $\Delta_9H_{\text{obs}} - \Delta_6H_{\text{obs}} = -22 \text{ kcal mol}^{-1}$  would have been expected; experimentally  $-43 \text{ kcal mol}^{-1}$  has been obtained (Table 1), while for recombination only  $\Delta_9H_{\text{obs}} - \Delta_6H_{\text{obs}} = -52 \text{ kcal mol}^{-1}$ . The following enthalpies data ( $\text{kcal mol}^{-1}$ ) are used:  $\Delta_f H_{298}$  (triethylamine)<sup>23</sup> =  $-22.1$ , BDE(R–H) = 89 (Table 1),  $\Delta_f H_{298}$  (1-(diethylamino)ethyl)<sup>23</sup> = 14.8,  $\Delta_f H_{298}$  (diethylvinylamine)<sup>23</sup> = 3.2 (using the increment of ethylamine to vinylamine of 25.3),  $\Delta_f H_{298}(\text{HO}_2\cdot) = 0.5$ , BDE(R–OO) = 30 (from Table 2).
- (35) Assuming that only eq 3 is operative,  $\Delta_9H_{\text{obs}} - \Delta_6H_{\text{obs}} = -17 \text{ kcal mol}^{-1}$  would have been expected; experimentally  $-13 \text{ kcal mol}^{-1}$  has been obtained (Table 1), while for recombination only  $\Delta_9H_{\text{obs}} - \Delta_6H_{\text{obs}} = -48 \text{ kcal mol}^{-1}$ . The following enthalpy data ( $\text{kcal mol}^{-1}$ ) are used:  $\Delta_f H_{298}$  (pyrrolidine)<sup>23</sup> =  $-0.8$ , BDE(R–H) = 87 (Table 1),  $\Delta_f H_{298}$  (1-pyrrolidinyl)<sup>23</sup> = 34.1,  $\Delta_f H_{298}$  (2-*H*-3,4-dihydropyrrole)<sup>23</sup> = 25.3. With DFT an increment of  $9.9 \text{ kcal mol}^{-1}$  is found, leading to  $\Delta_f H_{298}$  (2,3-dihydropyrrole) = 25.2, and BDE(R–OO) = 28 (from Table 2).